Electronic Supplementary Material (ESI) for Environmental Science: Processes & Impacts.
This journal is © The Royal Society of Chemistry 2024

Supporting information

Atmospheric mercury uptake and accumulation in forests dependent on climatic factors

Yo Han Yang[a], Min-Seob Kim[b], Jaeseon Park[b], Sae Yun Kwon[a*]

[a]Division of Environmental Science and Engineering, Pohang University of Science and Technology, 77 Cheongam-Ro, Nam-Gu, Pohang 37673, South Korea

[b]Environmental Measurement & Analysis Center, National Institute of Environmental Research, 42 Hwangyong-Ro, Seo-Gu, Incheon 22689, South Korea

* Corresponding author: Sae Yun Kwon
Phone: +82-54-279-2290
Fax: +82-54-279-8299
Email: saeyunk@postech.ac.kr

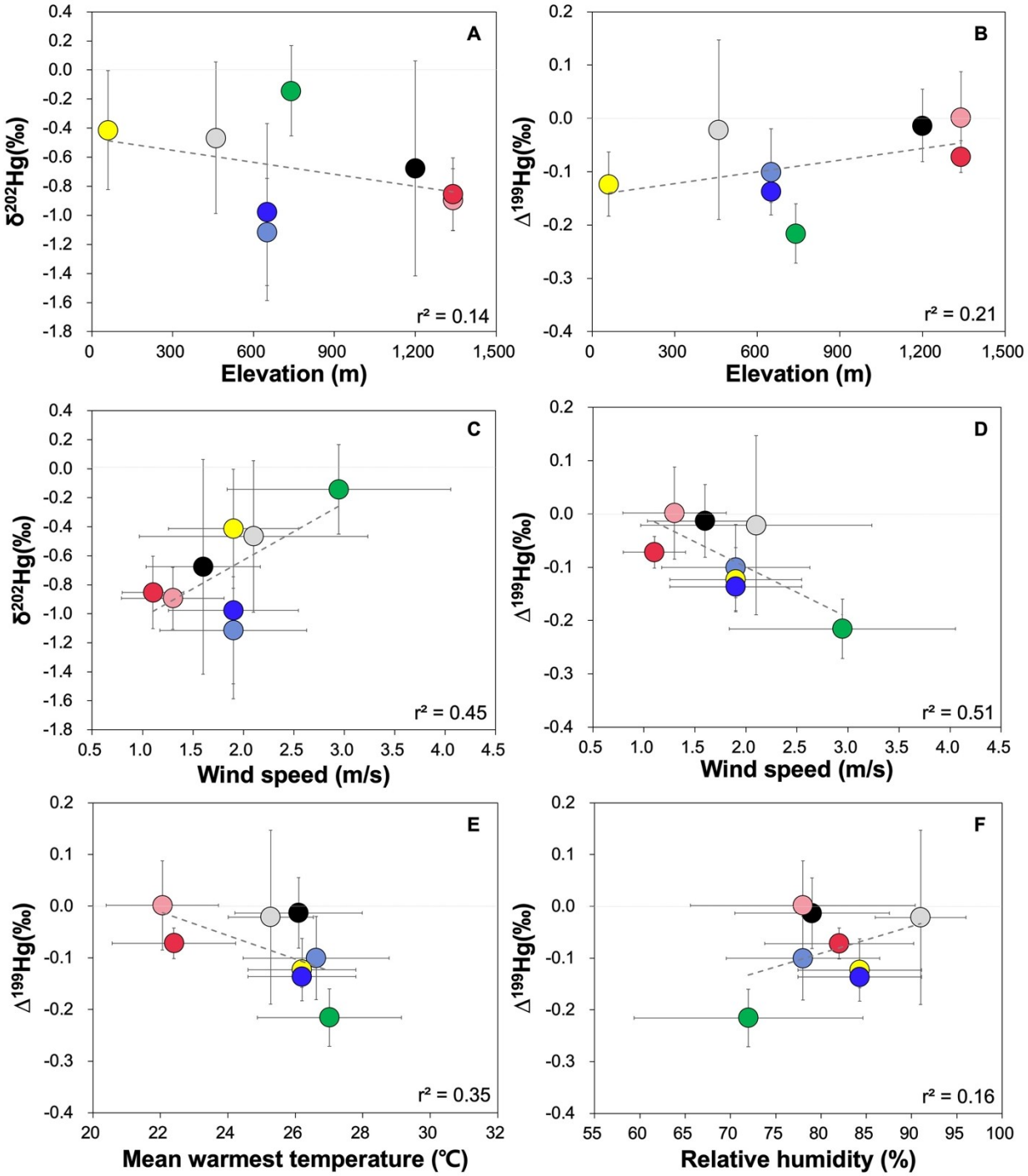

Figure S1. Site-specific average δ^{202}Hg values of TGM in relation to elevation (A) and wind speed (C). Site-specific average Δ^{199}Hg values of TGM in relation to elevation (B), wind speed (D), mean warmest temperature (E), and relative humidity (F).

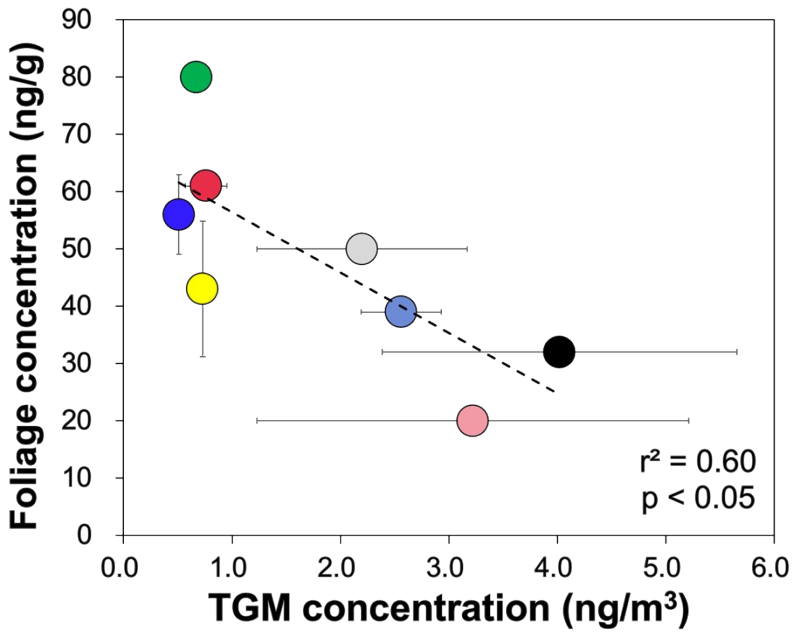

Figure S2. Site-specific average foliage THg concentration in relation to TGM concentration. The colors represent individual mountain site and are consistent with Figure 2.

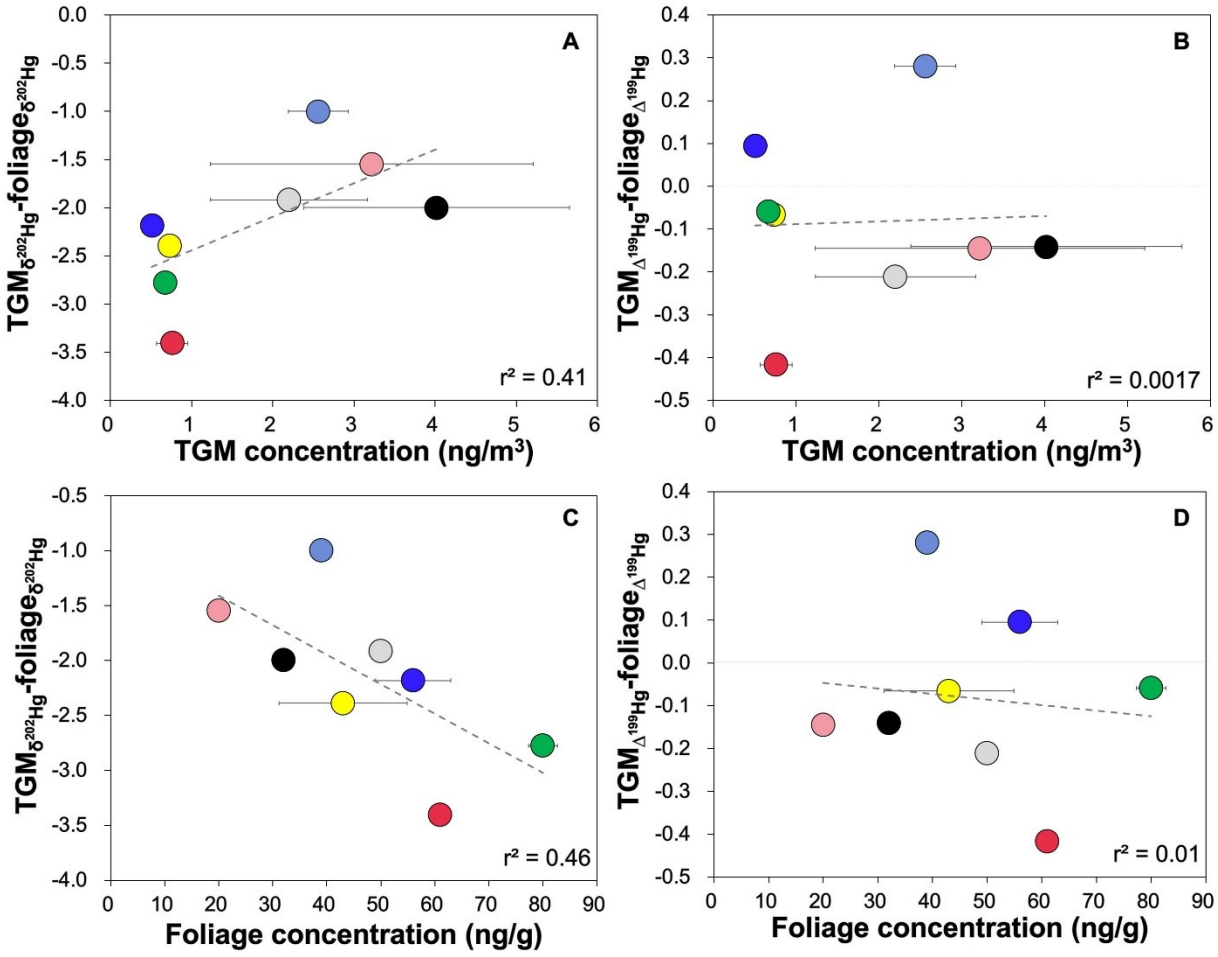

Figure S3. Site-specific average TGM concentration in relation to the magnitude of δ^{202}Hg shift from TGM to foliage (A) and Δ^{199}Hg shift from TGM to foliage (B). Site-specific average foliage THg concentration in relation to the magnitude of δ^{202}Hg shift from TGM to foliage (C) and Δ^{199}Hg shift from TGM to foliage (D). The colors represent individual mountain site and are consistent with Figure 2.

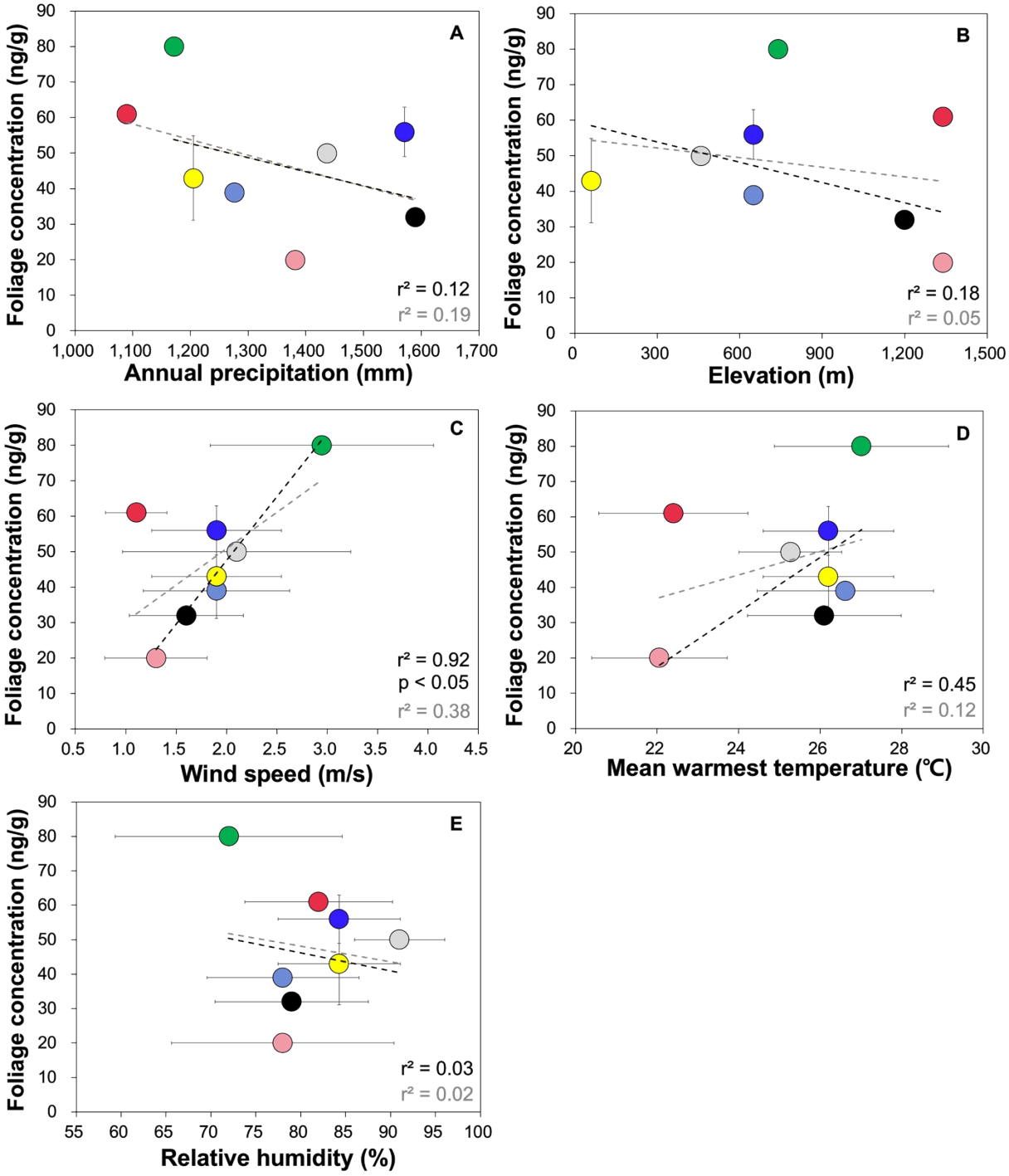

53

54 Figure S4. Site-specific average foliage THg concentration in relation to A) annual precipitation,
55 b) elevation, C) wind speed, D) mean warmest temperature, and E) relative humidity.

56

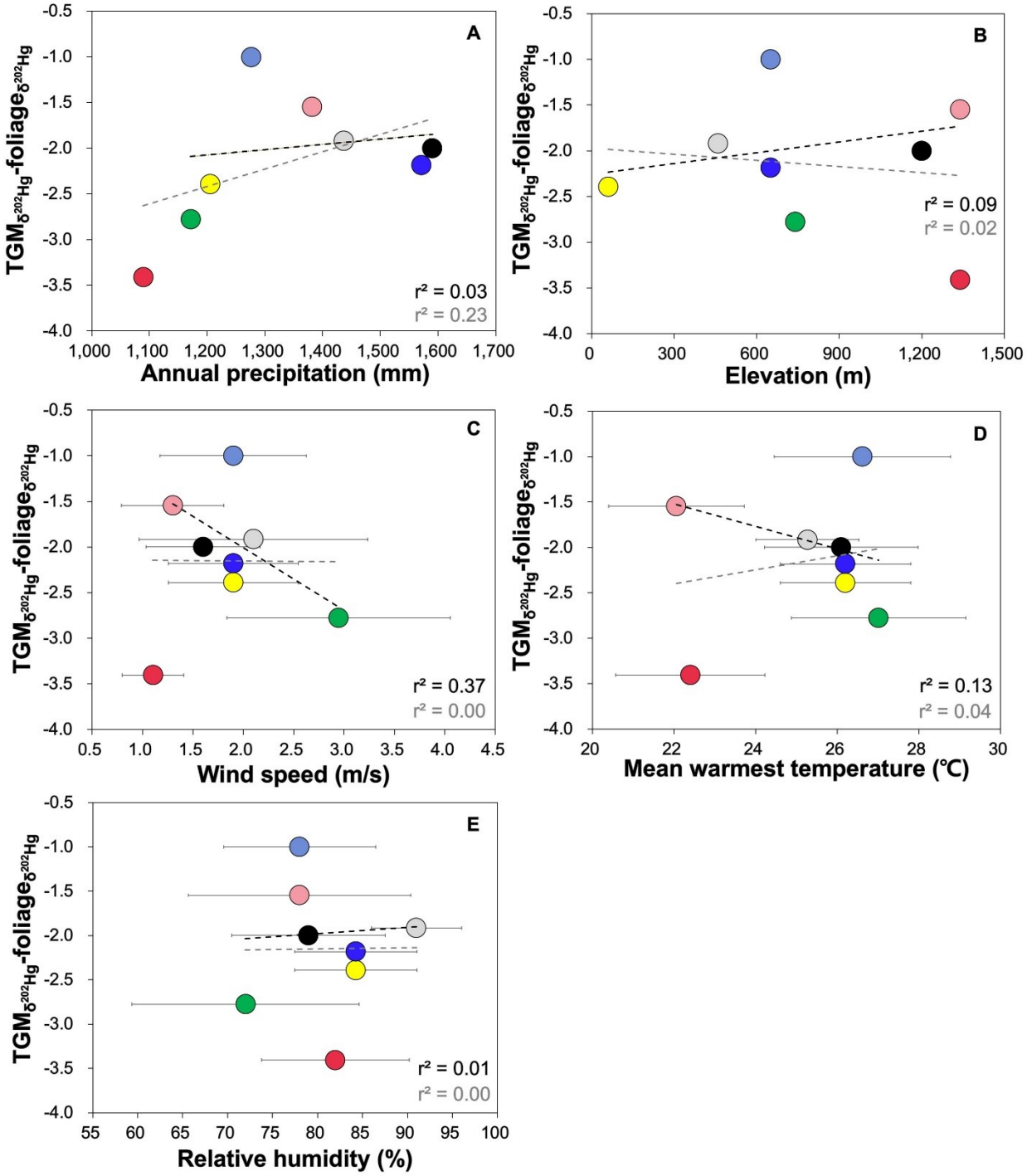

57

58 Figure S5. Magnitude of δ^{202}Hg shift from TGM to foliage in relation to A) annual precipitation,
59 b) elevation, C) wind speed, D) mean warmest temperature, and E) relative humidity of each
60 mountain site of South Korea.

61

62

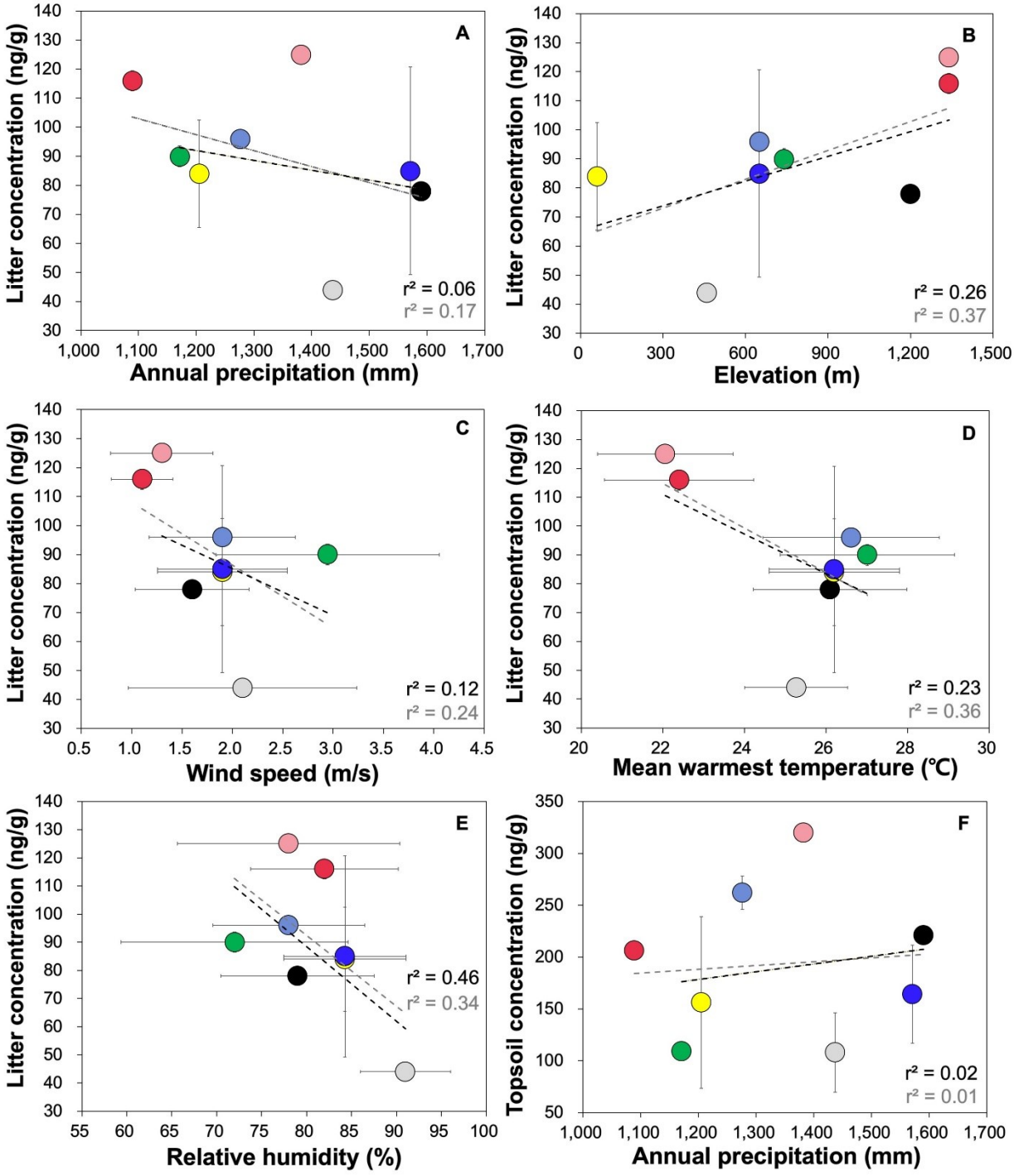
A
Litter concentration (ng/g)
Annual precipitation (mm)
r² = 0.06
r² = 0.17
B
Litter concentration (ng/g)
Elevation (m)
r² = 0.26
r² = 0.37
C
Litter concentration (ng/g)
Wind speed (m/s)
r² = 0.12
r² = 0.24
D
Litter concentration (ng/g)
Mean warmest temperature (°C)
r² = 0.23
r² = 0.36
E
Litter concentration (ng/g)
Relative humidity (%)
r² = 0.46
r² = 0.34
F
Topsoil concentration (ng/g)
Annual precipitation (mm)
r² = 0.02
r² = 0.01

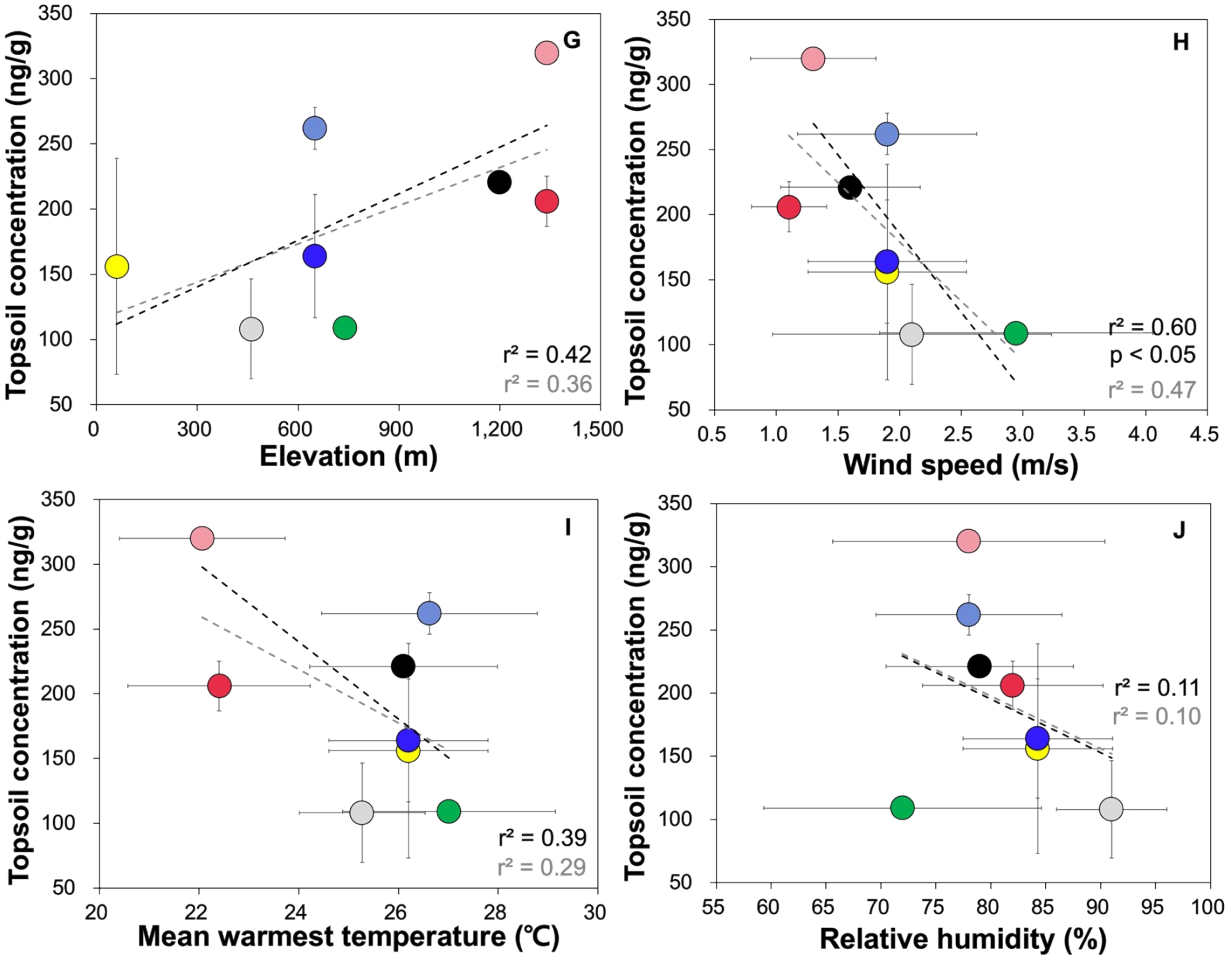

Figure S6. Site-specific average litter THg concentration in relation to A) annual precipitation, b) elevation, C) wind speed, D) mean warmest temperature, and E) relative humidity. Site-specific average topsoil THg concentration in relation to F) annual precipitation, G) elevation, H) wind speed, I) mean warmest temperature, and J) relative humidity.

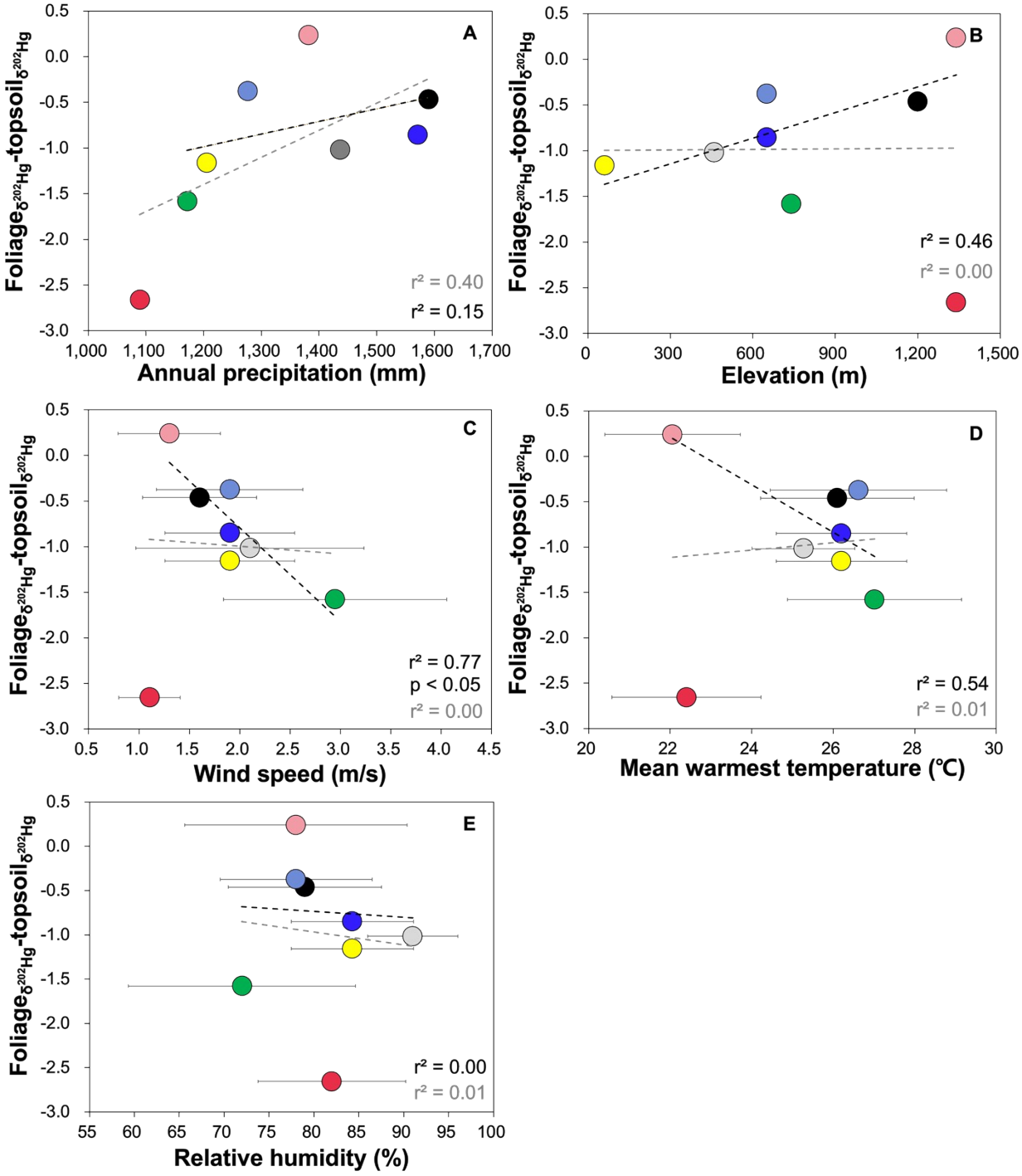

78

79 Figure S7. Magnitude of δ^{202}Hg shift from foliage to topsoil in relation to A) annual precipitation,
80 b) elevation, C) wind speed, D) mean warmest temperature, and E) relative humidity of each
81 mountain site of South Korea.

82 Table S1. Locations and climatic/environmental information of six mountain sites.

Site	Description	Sample year	Latitude	Latitude	Elevation (m asl)	Humidity (%)	Mean warmest temperature (°C)	Annual precipitation (mm)	Wind speed (m/s)
Bihak	East coast, adjacent to a steel complex	2019	36°15′N	129°23′E	740	72	27	1171	2.9
Mani	West coast, adjacent to regions of dense coal fired power plants	2020	36°62′N	126°43′E	460	91	25.3	1437	2.1
Hambaek	East coast, adjacent to a smelter	2021, 2022	37°16′N	128°92′E	1340	78, 82	22.6, 22.4	1382, 1089	1.3, 1.1
Jiri	Inland, no pollution source within a 50 km radius	2021	35°36′N	127°52′E	1200	79	26.1	1590	1.6
Gaya	West coast, adjacent to regions of dense coal fired power plants	2021, 2022	36°70′N	126°61′E	650	78, 84	26.6, 26.2	1276, 1571	1.9, 1.9
Seokmun	West coast, adjacent to	2022			60	84	26.2	1205	1.9

	regions of coal fired power plants

Table S2. Hg isotope ratios of standard reference materials measured in this study and other studies.

SRM	Sample type	n	δ^{202}Hg	2σ	Δ^{201}Hg	2σ	Δ^{200}Hg	2σ	Δ^{199}Hg	2σ	Reference
ERM CE 464	Tuna fish	1	0.56	-	1.86	-	0.08	-	2.31	-	This study
		3	0.66	0.08	1.91	0.06	-	-	2.31	0.09	Kwon *et al.*[1]
		3	0.71	0.08	1.89	0.05	0.09	0.08	2.28	0.11	Jung *et al.*[2]
		47	0.68	0.01	1.97	0.01	0.08	0.01	2.40	0.01	Blum and Johnson[3]
		3	0.71	0.03	2.00	0.03	0.08	0.01	2.40	0.01	
		10	0.70	0.14	1.96	0.10	0.08	0.08	2.37	0.14	Lee *et al.*[4]
TORT-3	Lobster	4	0.04	0.02	0.49	0.06	0.05	0.01	0.62	0.03	This study
		3	0.06	0.08	0.50	0.07	0.06	0.02	0.63	0.10	Jung *et al.*[2]
		4	0.07	0.04	0.55	0.08	0.06	0.06	0.67	0.05	Blum and Johnson[3]
		10	0.06	0.06	0.59	0.11	0.07	0.06	0.72	0.07	Enrico *et al.*[5]
		4	0.05	0.08	-	-	-	-	0.66	0.04	Croizier *et al.*[6]
		6	0.09	0.16	-	-	-	-	0.65	0.06	Croizier *et al.*[7]
NIST 2711a	Soil	5	-0.08	0.05	-0.18	0.02	-0.02	0.01	-0.23	0.01	This study
		3	-0.13	0.12	-0.17	0.06	-0.05	0.08	-0.24	0.02	Jung *et al.*[8]
		3	-	-	-0.18	0.06	-0.03	0.09	-0.25	0.09	Grigg *et al.*[9]
		6	-0.23	0.06	-0.19	0.05	0.00	0.03	-0.20	0.05	Liu *et al.*[10]
NIST RM 8610	Standard solution	40	-0.53	0.04	-0.03	0.02	0.01	0.01	-0.02	0.01	This study
		40	-0.54	0.11	-0.03	0.06	0.01	0.09	-0.01	0.12	Jung *et al.*[2]
		6	-0.54	0.09	-0.02	0.08	0.00	0.07	-0.01	0.05	Jung *et al.*[8]

88	-0.53	0.05	-0.04	0.03	0.01	0.03	-0.02	0.05	Lepak *et al.*[11]
42	-0.56	0.16	-	-	0.00	0.08	-0.02	0.08	Lee *et al.*[12]
403	-0.57	<0.005	-0.04	<0.005	0.01	<0.005	-0.02	<0.005	Blum and Johnson,[10]
34	-0.58	0.06	-0.04	0.04	0.02	0.04	-0.02	0.05	Demers *et al.*[13]

Table S3. Total gaseous mercury (TGM) concentration and Hg isotope ratios from six mountain sites.

Sites	Sample year	Concentration (ng/m^3)	δ^{202}Hg (‰)	Δ^{199}Hg (‰)	Δ^{200}Hg (‰)	Δ^{201}Hg (‰)	Δ^{204}Hg (‰)
Bihak	2019	0.55	-0.50	-0.28	-0.07	-0.25	-0.41
Bihak	2019	0.72	0.03	-0.19	-0.06	-0.12	-0.19
Bihak	2019	0.74	0.04	-0.17	-0.10	-0.22	-0.16
Mani	2020	1.49	-0.35	-0.10	-0.03	-0.07	0.07
Mani	2020	1.82	-0.02	-0.13	-0.05	-0.07	0.03
Mani	2020	3.30	-1.04	0.17	0.01	0.16	-0.01
Hambaek	2021	3.27	-0.91	-0.07	-0.03	-0.01	0.04
Hambaek	2021	6.01	-1.06	0.13	0.02	0.06	-0.02
Hambaek	2021	1.93	-1.01	-0.03	-0.02	-0.08	0.04
Hambaek	2021	1.67	-0.59	-0.03	-0.01	-0.09	0.04
Jiri	2021	3.44	-0.77	-0.08	-0.03	-0.11	0.08
Jiri	2021	2.76	-1.37	-0.02	-0.02	-0.05	0.03
Jiri	2021	5.87	0.10	0.06	-0.01	-0.01	0.04
Gaya	2021	2.79	-0.69	-0.03	-0.02	-0.09	0.04

Gaya	2021	2.14	-1.32	-0.19	-0.03	-0.21	0.07
Gaya	2021	2.76	-1.33	-0.09	-0.04	-0.08	0.06
Gaya	2022	0.65	-1.28	-0.13	-0.03	-0.32	0.14
Gaya	2022	0.61	-1.01	-0.12	-0.07	-0.42	0.18
Gaya	2022	0.39	-0.12	-0.12	-0.06	-0.50	0.25
Gaya	2022	0.40	-1.51	-0.17	-0.10	-0.82	0.44
Seokmun	2022	0.72	-0.26	-0.18	-0.06	-0.14	0.11
Seokmun	2022	0.76	-0.43	-0.15	-0.05	-0.19	0.12
Seokmun	2022	0.82	0.00	-0.11	-0.05	-0.19	0.05
Seokmun	2022	0.60	-0.97	-0.04	-0.04	-0.42	0.31
Hambaek	2022	0.80	-1.09	-0.07	-0.03	-0.19	0.18
Hambaek	2022	0.74	-0.98	-0.04	0.01	-0.20	0.16
Hambaek	2022	0.99	-0.52	-0.11	-0.04	-0.13	0.12
Hambaek	2022	0.52	-0.83	-0.70	0.00	-0.20	0.11

Table S4. Total Hg (THg) concentration and Hg isotope ratios of all solid samples (foliage, litter, topsoil) from six mountain sites. N_1 denotes the number of analyses for THg concentration and N_2 denotes the number of analyses for Hg isotopes.

Site	N_1	Average THg (ng/g)	1σ	N_2	δ^{202}Hg (‰)	1σ	Δ^{199}Hg (‰)	1σ	Δ^{200}Hg (‰)	1σ	Δ^{201}Hg (‰)	1σ	Δ^{204}Hg (‰)	1σ
Bihak 2019														
Foliage	3	80	2	3	-2.29	0.49	-0.27	0.02	0.00	0.01	-0.23	0.01	0.02	0.01
Litter	3	90	3	1	-2.50		-0.25		-0.02		-0.37		0.06	
Topsoil	3	109	3	1	-1.34		-0.21		0.01		-0.22		-0.02	
Mani 2020														
Foliage	3	50	1	3	-2.38	0.17	-0.23	0.02	-0.02	0.01	-0.07	0.19	0.03	0.03
Litter	3	44	1	3	-2.19	0.16	-0.20	0.01	0.01	0.02	-0.20	0.03	0.01	0.02
Topsoil	3	108	38	2	-1.37	0.01	-0.16	0.02	0.00	0.01	-0.15	0.02	0.02	0.01
Hambaek 2021														
Foliage	3	20	0	1	-2.44	-	-0.14	-	0.00	-	-0.13	-	0.01	-
Litter	3	125	2	3	-2.60	0.09	-0.21	0.02	-0.01	0.01	-0.22	0.02	0.01	0.01

Topsoil	3	320	4	3	-2.68	0.15	-0.19	0.01	0.02	0.00	-0.22	0.06	-0.01	0.03
Hambaek 2022														
Foliage	2	61	0.5	2	-4.26	0.29	-0.49	0.04	-0.06	0.00	-0.35	0.01	0.15	0.05
Litter	3	116	2	3	-3.01	0.11	-0.28	0.04	-0.02	0.02	-0.25	0.01	0.09	0.05
Topsoil	3	206	4	3	-1.60	0.14	-0.33	0.01	0.00	0.00	-0.36	0.01	-0.07	0.00
Jiri 2021														
Foliage	3	32	1	3	-2.67	0.14	-0.15	0.03	0.00	0.02	-0.15	0.02	0.02	0.02
Litter	3	78	2	3	-2.38	0.03	-0.21	0.03	-0.02	0.02	-0.19	0.01	0.05	0.01
Topsoil	3	221	7	3	-2.21	0.06	-0.23	0.00	0.01	0.01	-0.21	0.01	-0.02	0.00
Gaya 2021														
Foliage	3	39	1	3	-2.11	0.07	0.18	0.03	0.01	0.02	0.15	0.04	0.03	0.02
Litter	3	96	2	3	-2.31	0.02	-0.07	0.02	-0.03	0.02	-0.04	0.03	0.04	0.01
Topsoil	3	262	16	3	-1.74	0.02	-0.25	0.01	0.01	0.00	-0.24	0.01	-0.01	0.00
Gaya 2022														
Foliage	2	56	1	2	-3.16	0.12	-0.04	0.06	-0.07	0.00	-0.02	0.04	0.00	0.01

Litter	3	85	2	3	-2.51	0.10	-0.06	0.01	-0.02	0.02	-0.08	0.01	0.04	0.05
Topsoil	3	164	16	3	-2.31	1.31	-0.06	0.24	0.03	0.01	-0.09	0.25	0.01	0.06
Seokmun 2022														
Foliage	3	43	5	3	-2.80	0.22	-0.19	0.01	-0.03	0.01	-0.18	0.01	0.07	0.02
Litter	3	84	2	3	-2.44	0.29	-0.15	0.02	-0.01	0.02	-0.23	0.05	-0.01	0.07
Topsoil	3	156	16	3	-1.65	0.07	-0.27	0.03	0.01	0.01	-0.31	0.03	0.01	0.03

Table S5. Fractions of two Hg sources (end-members; Hg^0 and Hg^{2+}) in the all solid samples (foliage, litter, topsoil) from six mountain sites. The average $\Delta^{200}Hg$ of our TGM and the average $\Delta^{200}Hg$ of precipitation sampled from various regions of the world.[14-25]

Sites	Foliage		Litter		Topsoil	
	Hg^0	**Hg^{2+}**	**Hg^0**	**Hg^{2+}**	**Hg^0**	**Hg^{2+}**
Jiri 2021	0.82	0.18	0.92	0.08	0.75	0.25
Hambaek 2021	0.84	0.16	0.85	0.15	0.73	0.27
Gaya 2021	0.76	0.24	0.98	0.02	0.75	0.25
Mani 2020	0.93	0.07	0.78	0.22	0.84	0.16
Hambaek 2022	1.12	-0.12	0.92	0.08	0.80	0.20
Seokmun 2022	0.96	0.04	0.87	0.13	0.74	0.26
Bihak 2019	0.82	0.18	0.89	0.11	0.78	0.22
Gaya 2022	1.17	-0.17	0.92	0.08	0.69	0.31

References

1. S. Y. Kwon, J. D. Blum, C. Y. Chen, D. E. Meattey and R. P. Mason, Mercury isotope study of sources and exposure pathways of methylmercury in estuarine food webs in the Northeastern US, *Environ. Sci. Technol.*, 2014, **48**, 10089–10097.

2. S. Jung, S. Y. Kwon, M.-L. Li, R. Yin and J. Park, Elucidating sources of mercury in the west coast of Korea and the Chinese marginal seas using mercury stable isotopes, *Sci. Total Environ.*, 2022, **814**, 152598.

3. J. D. Blum and M. W. Johnson, Recent Developments in Mercury Stable Isotope Analysis, *Rev. Mineral. Geochem.*, 2017, **82**, 733–757.

4. B. J. Lee, S. Y. Kwon, R. Yin, M. Li, S. Jung, S. H. Lim, J. H. Lee, K. W. Kim, K. D. Kim and J. W. Jang, Internal dynamics of inorganic and methylmercury in a marine fish: Insights from mercury stable isotopes, *Environ. Pollut.*, 2020, **267**, 115588.

5. M. Enrico, P. Balcom, D. T. Johnston, J. Foriel and E. M. Sunderland, Simultaneous combustion preparation for mercury isotope analysis and detection of total mercury using a direct mercury analyzer, *Anal. Chim. Acta,* 2021, **1154**, 338327.

6. G. L. Croizier, A. Lorrain, J. E. Sonke, S. Jaquemet, G. Schaal, M. Renedo, L. Besnard, Y. Cherel and D. Point, Mercury isotopes as tracers of ecology and metabolism in two sympatric shark species, *Environ. Pollut.*, 2020, **265**, 114931

7. G. L. Croizier, A. Lorrain, J. E. Sonke, E. M. Hoyos-Padila, F. Galván-Magaña, O. Santana-Morales, M. Aquino-Baleytó, E. E. Becerril-García, G. Muntaner-López, J. Ketchum, B. Block, A. Carlisle, S. J. Jorgensen, L. Besnard, A. Jung, G. Schaal and D. Point, The twilight zone as a major foraging habitat and mercury source for the great white shark, *Environ. Sci. Technol.*, 2020, **54**, 15872-15882.

8. S. Jung, S. Y. Kwon, Y. Hong, R. Yin and L. C. Motta, Isotope investigation of mercury sources in a creek impacted by multiple anthropogenic activities, *Chemosphere*, 2021, **282**, 130947.

9. A. R., Grigg, R. Kretzschmar, R. S. Gilli and J. G. Wiederhold, Mercury isotope signatures of digests and sequential extracts from industrially contaminated soils and sediments, *Sci. Total Environ.*, 2018, **636**, 1344-1354.

10. C. Liu, X. Fu, Y. Xu, H. Zhang, X. Wu, J. Sommar, L. Zhang, X. Wang and X. Feng, Sources and transformation mechanisms of atmospheric particulate bound mercury revealed by mercury stable isotopes, *Environ. Sci. Technol.*, 2022, **56**, 5224-5233.

11. R. F, Lepak, S. E. Janssen, D. R. Engstrom, D. P. Krabbenhoft, M. T. Tate, R. Yin, W. F. Fitzgerald, S. A. Nagorski and J. P. Hurley, Resolving atmospheric mercury loading and source trends from isotopic records of remote North American lake sediments, *Environ. Sci. Technol.*, 2020, **54**, 9325-9333.

12. J. H. Lee, S. Y. Kwon, H. Lee, S.-I. Nam, J.-H. Kim, Y. J. Joo, K. Jang, H. Kim and R. Yin, Climate-associated changes in mercury sources in the arctic fjord sediments, *ACS Earth Space Chem.*, 2021, **5**, 2398−2407.

13. J. D. Demers, J. D. Blum, S. C. Brooks, P. M. Donova, A. L. Riscassi, C. L. Miller, W. Zheng and B. Gu, Hg isotopes reveal in-stream processing and legacy inputs in East Fork Poplar Creek, Oak Ridge, Tennessee, USA, *Environ. Sci. Process Impacts*, 2018, **20**, 686-707.

14. Demers, J.D., Blum, J.D., Zak, D.R., 2013. Mercury isotopes in a forested ecosystem: implications for air-surface exchange dynamics and the global mercury cycle. Glob. Biogeochem. Cycles 27 (1), 222–238. https://doi.org/10.1002/gbc.20021.

15. Yuan, S., Zhang, Y., Chen, J., Kang, S., Zhang, J., Feng, X., Cai, H., Wang, Z., Wang, Z., Huang, Q., 2015. Large variation of mercury isotope composition during a single precipitation event at Lhasa City, Tibetan Plateau, China. Proced. Earth Plan. Sci. 13, 282–286. https://doi.org/10.1016/j.proeps.2015.07.066.

16. Chen, J., Hintelmann, H., Feng, X., Dimock, B., 2012. Unusual fractionation of both odd and even mercury isotopes in precipitation from Peterborough, ON, Canada. Geochim. Cosmochim. Acta 90, 33–46. https://doi.org/10.1016/j.gca.2012.05.005.

17. Donovan, P.M., Blum, J.D., Yee, D., Gehrke, G.E., Singer, M.B., 2013. An isotopic record of mercury in San Francisco Bay sediment. Chem. Geol. 349, 87–98. https://doi.org/

10.1016/j.chemgeo.2013.04.017.

18. Sherman, L.S., Blum, J.D., Keeler, G.J., Demers, J.D., Dvonch, J.T., 2012. Investigation of local mercury deposition from a coal-fired power plant using mercury isotopes. Environ. Sci. Technol. 46 (1), 382–390. https://doi.org/10.1021/es202793c.

19. Sherman, L.S., Blum, J.D., Dvonch, J.T., Gratz, L.E., Landis, M.S., 2015. The use of Pb, Sr, and Hg isotopes in Great Lakes precipitation as a tool for pollution source attribution. Sci. Total Environ. 502, 362–374. https://doi.org/10.1016/j.scitotenv.2014.09.034.

20. Gratz, L.E., Keeler, G.J., Blum, J.D., Sherman, L.S., 2010. Isotopic composition and fractionation of mercury in Great Lakes precipitation and ambient air. Environ. Sci. Technol. (20), 7764–7770. https://doi.org/10.1021/es100383w.

21. Wang, Z., Chen, J., Feng, X., Hintelmann, H., Yuan, S., Cai, H., ... & Wang, F. (2015). Mass-dependent and mass-independent fractionation of mercury isotopes in precipitation from Guiyang, SW China. Comptes Rendus Geoscience, 347(7-8), 358-367.

22. Huang, S., Sun, L., Zhou, T., Yuan, D., Du, B., Sun, X., 2018. Natural stable isotopic compositions of mercury in aerosols and wet precipitations around a coal-fired power plant in Xiamen, southeast China. Atmos. Environ. 173, 72–80. https://doi.org/10.1016/j.atmosenv.2017.11.003.

23. Motta, L.C., Blum, J.D., Johnson, M.W., Umhau, B.P., Popp, B.N., Washburn, S.J., Drazen, J.C., Benitez-Nelson, C.R., Hannides, C.C.S., Close, H.G., Lamborg, C.H., 2019. Mercury cycling in the North Pacific Subtropical Gyre as revealed by mercury stable isotope ratios. Global Biogeochem. Cyc. 33, 777–794. https://doi.org/10.1029/ 2018GB006057.

24. Enrico, M., Roux, G.L., Marusczak, N., Heimbürger, L.E., Claustres, A., Fu, X., Sun, R., Sonke, J.E., 2016. Atmospheric mercury transfer to peat bogs dominated by gaseous elemental mercury dry deposition. Environ. Sci. Technol. 50, 2405–2412. https://doi.org/10.1021/acs.est.5b06058.

25. Fu, X., Jiskra, M., Yang, X., Marusczak, N., Enrico, M., Chmeleff, J., ... & Sonke, J. E. (2021). Mass-independent fractionation of even and odd mercury isotopes during atmospheric mercury redox reactions. Environmental science & technology, 55(14), 10164-10174.